esoc

European Space Operations Centre
Robert-Bosch-Strasse 5
D-64293 Darmstadt
Germany
T +49 (0)6151 900
F +49 (0)6151 90495
www.esa.int

DOCUMENT

MTGI1/NGRM Level 1 data description

MTGI1/NGRM Level 1 datasets

Prepared by **Ingmar Sandberg**
Space Applications & Research Consultancy
Reference **SPARC-MTGI1-NGRM-L1 Data Description**
Issue/Revision **1.0**
Date of Issue **18/06/2025**
Status **Completed**

APPROVAL

Title MTGI1/NGRM Level 1 datasets	
Issue Number 1	**Revision Number** 0
Authors Ingmar Sandberg	**Date** 18/06/2025
Approved By	**Date of Approval**

CHANGE LOG

Reason for change	Issue Nr.	Revision Number	Date

DISTRIBUTION

Name/Organisational Unit

Ingmar Sandberg

Digitally signed by Ingmar Sandberg
Date: 2025.06.23 12:10:47 +03'00'

Digitally signed by Melanie Heil
Date: 2025.06.25 11:48:19 +02'00'

Table of contents:

Table of figures:

Table of tables:

1 REFERENCE DOCUMENTS AND ACRONYMS

1.1 Reference Documents

[RD 1] L. Desorgher, W. Hajdas, I. Britvitch, K. Egli, X. Guo, Y. Luo, F. Chastellain, C. Pereira, R. Muff, D. Boscher, G. Maehlum, and D. Meier, “The next generation radiation monitor- NGRM,” in 2013 IEEE Nuclear Science Symposium and Medical Imaging Conference (2013 NSS/MIC). IEEE, Oct. 2013, pp. 1–6.

[RD 2] SSA P3-SWE-XXI - NGRM Data Processing, TN7: MTG I1/NGRM extended response functions, Reference: SE2S-NGRM-TN7

[RD 3] S. Agostinelli et al., “Geant4—a simulation toolkit,” Nuclear Instruments and Methods in Physics Research Section A: Accelerators, Spectrometers, Detectors and Associated Equipment, vol. 506, no. 3, pp. 250–303, Jul.2003.

[RD 4] I. Sandberg et al., "Data Exploitation of New Galileo Environmental Monitoring Units," in IEEE Transactions on Nuclear Science, vol. 66, no. 7, pp. 1761-1769, July 2019

[RD 5] S. Aminalragia-Giamini et al 2018, Artificial intelligence unfolding for space radiation monitor data, J. Space Weather Space Clim. 2018, 8, A50, https://doi.org/10.1051/swsc/2018041

[RD 6] A. Boudouridis, J. Rodriguez, B. Kress, B. Dichter, and T. Onsager, “Development of a bowtie inversion technique for real-time processing of the GOES-16/-17 SEISS MPS-HI electron channels,” Space Weather, vol. 18, no. 4, Apr. 2020.

[RD 7] SEPEM reference data set (rds) v2.X 2017a, http://test.sepem.eu/help/SEPEM RDS v2-00.zip

[RD 8] I. Sandberg, P. Jiggens, D. Heynderickx, and I. A. Daglis, “Cross calibration of NOAA GOES solar proton detectors using corrected NASA IMP-8/GME data”, Geophysical Research Letters, vol. 41, no. 3, pp. 4435- 4441, 2014d

[RD 9] Sandberg et al, “First results and analysis from ESA Next Generation Radiation Monitor unit on-board EDRS-C”, IEEE Transactions on Nuclear Science. 10.1109/TNS.2022.3160108

[RD 10] UNILIB http://www.mag-unilib.eu/

1.2 Acronyms

Acronyms used in this document and needing a definition can be found in:

Acronym	Definition
AI	Artificial Intelligence
BT	Bow-Tie
CBR	Case-Based-Reasoning
EDRS-C	European Data Relay Satellite C
ESA	European Space Agency
EDSS	Electron Detector Stacked System
ESOC	European Space Operations Centre
ESTEC	European Space Research and Technology Centre
GA	Genetic Algorithm
GenCORUM	Genetic Correlative Unfolding Method
GEO	Geosynchronous Orbit
GP	Ground Processor
FEDO	Omni-directional Differential Electron Flux
FEIO	Omni-directional Integral Electron Flux
FPDO	Omni-directional Differential Proton Flux
MPS-Hi	Magnetospheric Particle Sensor High (Energy)
MTG-I 1	Meteosat Third Generation-Imager 1
NGRM	Next Generation Radiation Monitor
RB	Radiation Belts
REM	Radiation Environment Monitor
RF	Response Function
SDSS	Solid Detector Stacked System
SEP	Solar Energetic Particle
TN	Technical Note

Table 1: Acronyms

2 INTRODUCTION

2.1 Purpose

This document describes the main characteristics of the released MTG-I1 (also known as Meteosat-12) NGRM Level 1 Version 1 datasets, and highlights the methods used for their derivation.

2.2 Background

ESA Next Generation Radiation Monitor (NGRM) was designed to measure protons from 2 MeV up to 200 MeV and electrons from 100 keV up to 7 MeV. NGRM development started within a consortium led by TAS-CH space (former RUAG space), together with Paul Scherrer Institute (PSI), Office National d'Etudes et de Recherches Aerospatiales (ONERA), EREMS, and Integrated Detector Electronics AS (IDEAS).

Meteosat Third Generation-Imager 1 (MTG-I 1), launched on 13 December 2022, is located at Geostationary orbit (GEO) and carries the third NGRM operating unit. The first unit was placed on-board the GEO European Data Relay System Satellite-C (EDRS-C), launched on August of 2019 and the second was placed on board the Low Earth Orbit (LEO) Sentinel-6 Michael Freilich (S6-MF) satellite, launched on November 2020.

Within "SSA P3-SWE-XXI NGRM Data Processing activity", SPARC led a consortium that included Solenix, SE2S and DHConsultancy, as external service provider, aiming to the design and the implementation of the NGRM Ground Processor. The performed developments included, among others, the derivation of the response functions for the NGRM units and the development and implementation of methods for the derivation of NGRM Level 1 flux products. The present document focuses on the NGRM unit on-board MTGI-1.

2.3 ESA NEXT GENERATION RADIATION MONITOR

The NGRM unit includes the electron and the stacked detector subsystems [RD 1] . The electron detector subsystem (EDSS) provides measurements in 16 channels while the stacked (proton) detector subsystem (SDSS) in 10 channels. EDSS is a circular strip detector made of 16 strips covered by a collimator made by an aluminium part on the bottom and covered by a copper cone on the top. The collimator is embedded in the aluminium housing acting as a field-of-view limiter and side shielding against particles coming from other directions. The aluminium part of the collimator is made by a concentric succession of 12 circular stairs with different thicknesses. Each silicon circular strip is bonded to an ASIC high gain channel where particles are counted when their deposited energy is within the range fixed by the low and high detection thresholds of the corresponding ASIC channel. SDSS consists of a stack of 7 Silicon cylindrical diodes separated by aluminium and tantalum degraders of different thicknesses. The diodes and the absorbers are shielded from the side by copper and aluminium cylinders. The aperture of the detector has a half opening angle of 40 degrees. Energetic particles coming from the top through the aperture cone are detected by ionization in a diode if they have sufficient minimum energy to cross all the previous degraders and diodes. The ionization current generated by a particle crossing the diode is processed by ASIC electronic circuits.

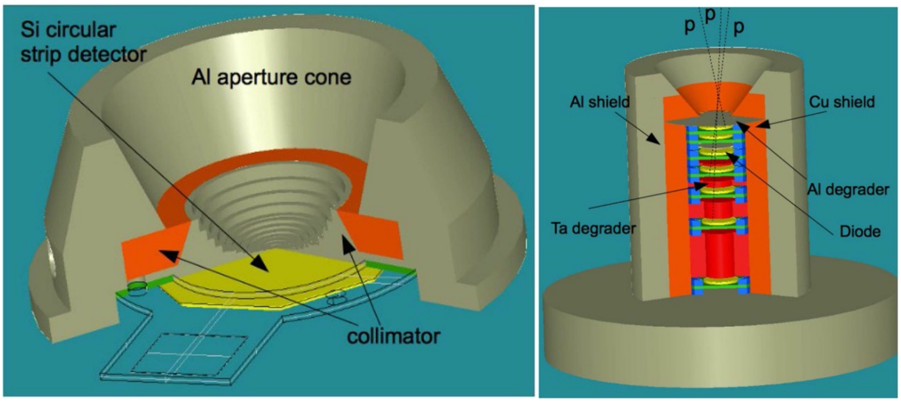

Figure 1: Model of the NGRM electron detector (left) and stacked detector (right).

3 CALIBRATION OF NGRM UNIT

The electron (proton) response functions (RF) of the EDSS (SDSS) of NGRM on-board MTGI1 have been derived [RD 2] on the basis of experimental and GEANT4 [RD 3] numerical calibrations. The response curves were numerically derived, and they were re-adjusted using the experimental results of the unit's experimental calibrations that took place at the Proton Irradiation and at the Electron Monochromator Facilities at Paul Scherrer Institute in Switzerland. The curves of the finalized response functions that were used for the calibration of the MTGI1/NGRM measurements and the derivation of the Level 1 flux products are presented below.

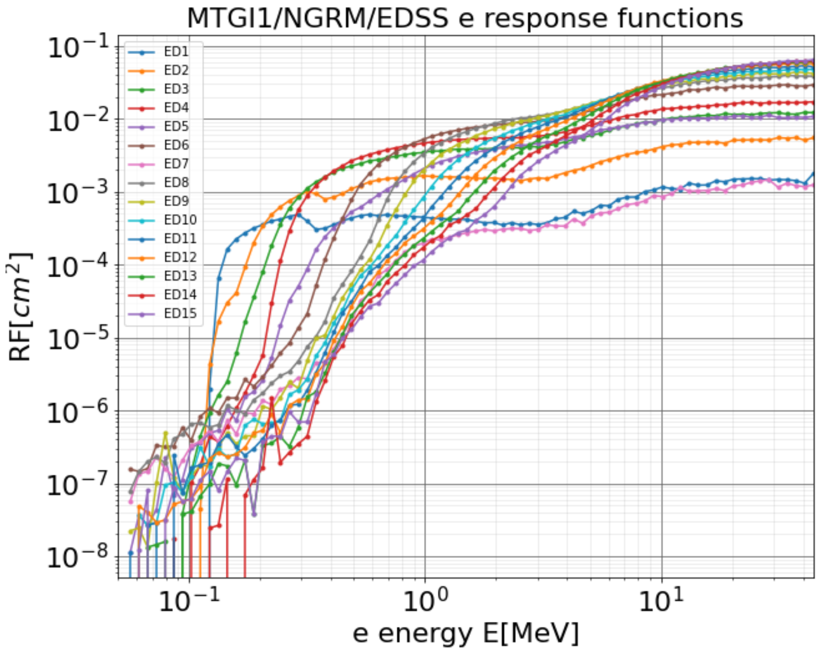

Figure 2: Omni-directional electron response functions of MTGI1/NGRM Electron Detector (ED) channels.

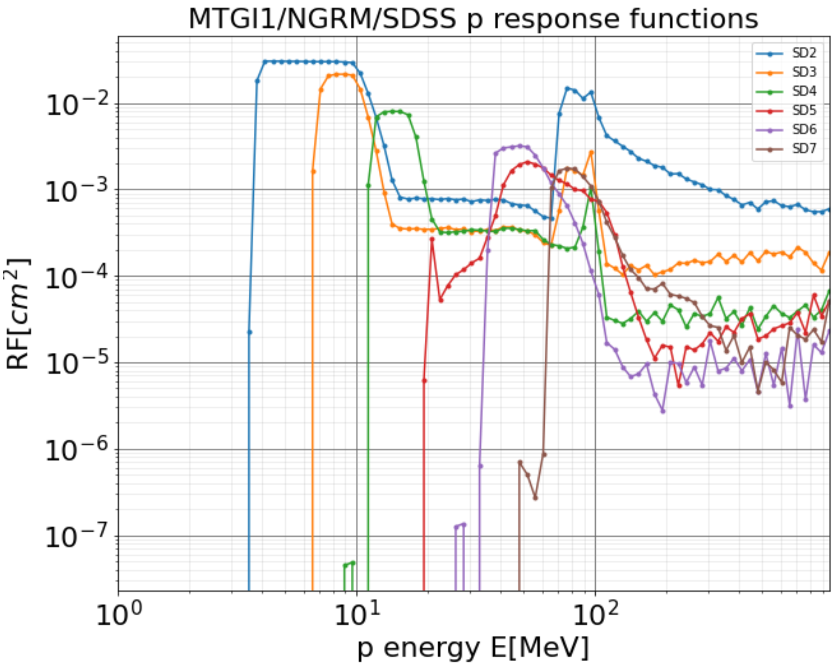

Figure 3: Omni-directional proton response function of MTGI1/NGRM Stacked Detector (SD) channels.

4 DATA CALIBRATION

The conversion of count data to calibrated energetic particle fluxes, corresponds to the derivation of solutions of the one-dimensional unfolding problem where the response (measurements) *C* of a detector is the result of the convolution of the incident differential particle fluxes *f(E)* with the response function *RF(E)* of the unit.

$$C = \int_0^\infty f(E)\, RF(E)\, dE \qquad \textbf{Equation 1}$$

For the derivation of MTGI1 NGRM Level-1 fluxes two different methodologies were employed. For the calculation of proton differential fluxes and electron integral fluxes, simple multiplicative scaling factors were derived and applied, using the Bow-Tie (BT) analysis [RD 4]. The BT analysis allows the derivation of a scaling factor for the conversion of the detector's count rates to flux products for an energy value that minimizes the uncertainties expected at the encountered space radiation environment. For the calculation of electron differential fluxes, the Genetic Correlative Unfolding Method (GenCORUM) was applied. The GenCORUM [RD 5] is an artificial intelligence method which employs a Cased-Based Reasoning (CBR) process coupled with a Genetic Algorithm (GA).

4.1 Electron Integral Flux Dataset: Level 1 Version 1

For the calculation of electron integral fluxes, a data-driven variant [RD 4] of the commonly used Bow-Tie (BT) analysis approach was implemented. For the sampling of electron radiation environment at GEO environment the differential electron flux measurements from MPS-HI [RD 6] detector on-board NOAA GOES 16 mission were used. The MPS-HI electron flux measurements were initially fitted, using a power law with an exponential

cutoff, and the resulting dataset, i.e. *f (E,t)* was used for the derivation of suitable NGRM scaling factors following the procedure below.
For each ED channel, distributions of geometric factors $GF(E_i, t)$ for different energies E_i were derived through the integration of the training differential flux spectra with the corresponding response function divided by the training integral flux spectra:

$$GF(E_i\,, t) = \frac{\int_0^\infty RF(E)\, f(E) dE}{\int_{Ei}^\infty f(E) dE} \qquad \textbf{Equation 2}$$

A characteristic bow-tie energy was determined for each channel as the optimum value that minimizes the mean squared error of the distribution of the logarithmic values of the geometric factors. The median value of the resulted distributions, $SF_{50}=1/median(GF(E_{BT}))$, was selected for the definition of the scaling factor for each channel.

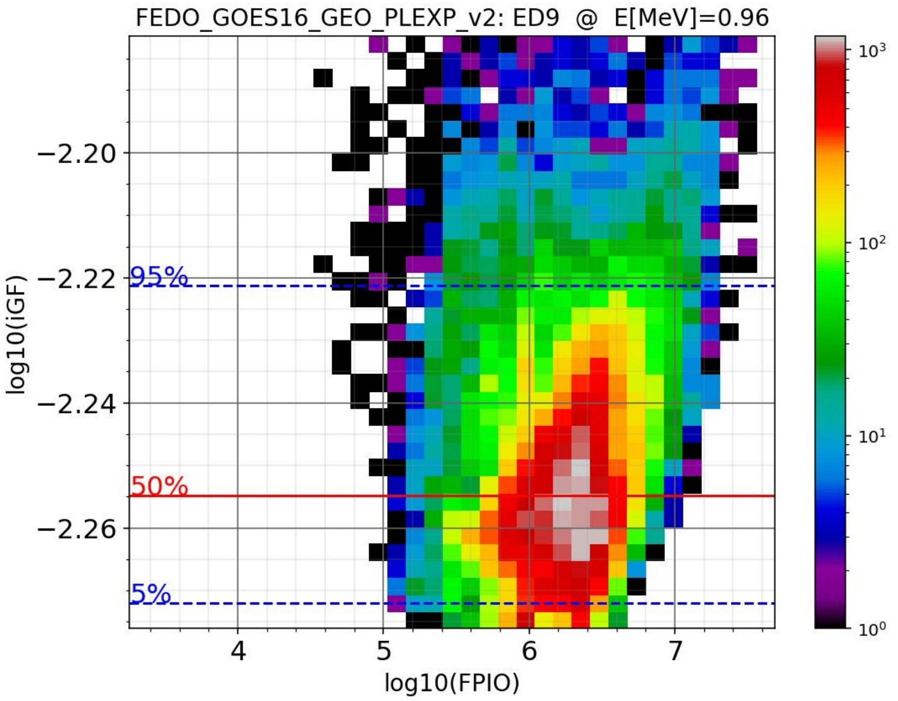

Figure 4: Histogram of the distribution of the geometric factors for ED9, derived using Equation 1. The horizonal lines denote selected percentiles of the geometric factors.

For a quantitative evaluation of the uncertainties of the derived electron flux which are attributed to the selection of the median value of the distribution of the geometric factors – as derived by using as sample measurements – we have calculated the uncertainties using the extremes in the sampled electron radiation environment measurements.

The table below summarizes the results associated to the derivation of the MTGI1 NGRM electron integral fluxes – based on selected ED channels - which have been introduced in the Level 1 Version 1 dataset.

The table includes also the relative differences between the 1% and the 99% percentiles of the scaling factor distributions with respect to the median value (50% percentile) which was used for the derivation of the integral electron fluxes.

Table 2: Characteristics of L1 V1 MTGI1/NGRM electron integral flux dataset.

Flux Bin	EDSS channel	FEIO_ENERGY [MeV]	SF50	(SF1-SF50)/SF1	(SF99-SF50)/SF99
1	2	0.2	1031	0.09	-0.12
2	3	0.3	405	0.03	-0.08
3	4	0.4	235	0.04	-0.13
4	6	0.6	186	0.03	-0.12
5	9	1.0	159	0.06	-0.17
6	11	1.1	319	0.08	-0.38
7	13	1.2	481	0.11	-0.45

The negative sign in the last column indicates an overestimation of the BT flux products with respect to the 0.99 percentile.

The calculation of the integral electron fluxes FEIO requires the application of the following scheme,

$$FEIO[FEIO_{ENERGY}] = \frac{SF_{50} \times ED_{COUNTRATE}}{4\pi} \; [cm^2 \sec str]^{-1} \qquad \textbf{Equation 3}$$

which takes place on-the-fly as soon as raw ED measurements become available at NGRM Ground Processor.

4.2 Proton Differential Flux Dataset: Level 1 Version 1

For the calculation of proton differential fluxes, a BT analysis of NGRM SDSS proton responses was applied using the Solar Energetic Particle Environment Modelling (SEPEM) reference dataset (SEPEM RDS) [RD 7] as a training dataset. SEPEM is based on NOAA GOES proton flux measurements cross-calibrated by [RD 8] using as reference the IMP-8 Goddard Medium Energy experiment.

In what follows we summarize the results of the BT analysis of the selected SD channels that were used for the creation of the proton differential flux products in Level 1 dataset.

Table 3: Characteristics of MTGI1/NGRM proton differential flux dataset.

Flux Bin	SDSS channels	FPDO Energy [MeV]	SF_50	(SF1-SF50)/SF1	(SF99-SF50)/SF99
1	2	5.5	6.4	0.005	-0.08
2	3	8.5	12.1	0.002	-0.03
3	4	14.5	18.8	0.003	-0.05
4	6	47.0	12.9	0.002	-0.03
5	7	80.0	16.2	0.003	-0.03

The calculation of the proton differential fluxes FPDO requires the application of the following scheme,

$$FPDO[FPDO_{ENERGY}] = \frac{SF_{50} \times SD_{COUNTRATE}}{4\pi}\ [cm^2 MeV\ \sec str]^{-1} \qquad \textbf{Equation 4}$$

which takes place on-the-fly as soon as raw SD measurements become available at NGRM Ground Processor.

As mentioned above, the scaling factors were derived to optimize the derivation of proton fluxes from SPEs.

4.3 Electron Differential Flux Dataset: Level 1 Version 1

The application of any direct re-scaling approach results to uncertainties in the derivation of differential particle fluxes. This is especially true for energies above 1 MeV in the case of NGRM units where the electron response functions are of integral-type. Thus, for the derivation of the electron differential fluxes, the GenCORUM method was adopted. GenCORUM is an artificial intelligence method which combines two different methodologies; a Case-Based-Reasoning (CBR) process and a Genetic Algorithm (GA). The CBR process performs an initial "rough" unfolding producing particle spectra and this output is forwarded to the GA which fine-tunes each spectrum independently producing the final unfolded particle fluxes.
During the CBR process, a virtual "library" is created by folding virtual electron flux spectra derived from an exponential cut-off power-law function with ED electron response functions and producing the counterpart virtual count-rates. Each count-rate measurement is correlated with the virtual library and the highest correlated virtual count-rate is found extracting its counter-part virtual flux as the match. Finally, a new intensity factor $\boldsymbol{a}$ is derived from a linear fitting of the measured and virtual count-rates. This new $\boldsymbol{a}$ is directly applied multiplicatively to the virtual flux to produce the unfolded spectrum, this is possible because a simple multiplicative change in the spectrum results in an equal change in the count-rate by definition (c.f. Equation 1). The unfolded spectrum is being used by a Genetic algorithms (GA) as an initial input. The GA is not bound by any strict analytical function offering much more versatility and potentially unfolded spectra that are much closer to reality. The GA process is depicted in the figure below. Each CBR spectrum corresponding to a measurement is randomly perturbed in order to create an initial population of N spectra that are similar but not identical.

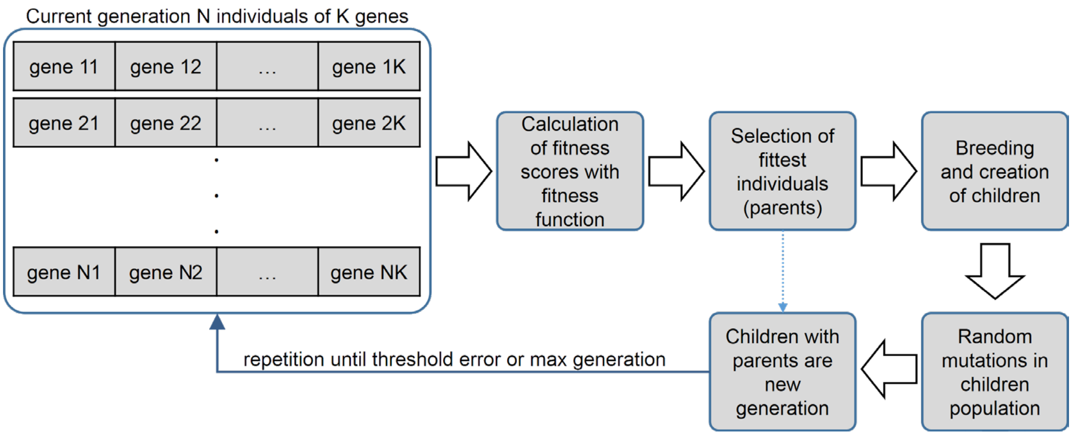

Figure 5: Diagram of the AI part of the GenCORUM process

The flux values at each energy bin are used as the "genes" in the algorithm. Each of the similar spectra is evaluated and scored in terms of how well it reconstructs the measured count-rate. The mean absolute percentage error (MAPE) is used as the fitness (score) function because it is not affected by the absolute values of the values in the count-rate vector which can often vary by many orders of magnitude.

The process consists of four main steps:
- Fitness evaluation of the population where all the spectra are scored
- Parent selection from the population where the best performing (highest score / lowest error) spectra are selected as "parents"
- Breeding and creation of children population where the selected parents are randomly combined to create again N "children" spectra
- Random mutation of the children spectra where some of the flux values are randomly perturbed

These steps create a new population, and they are iteratively repeated, each iteration is dubbed a generation. As generations progress the overall and best performance increases and the overall and lowest error decreases. The differential electron fluxes are calculated in near real-time - as soon as NGRM raw data become available - using a GenCORUM implementation and are provided in the energy bins listed in Table 4.

Table 4: Characteristics of MTGI1/NGRM electron differential flux dataset.

Flux Bin	FEDO_ENERGY [MeV]
1	0.18
2	0.27
3	0.40
4	0.60
5	0.88
6	1.30
7	1.93
8	2.90
9	3.40
10	4.00

NOTE: For the GenCORUM implementation NGRM channels ED2, ED3, ED4, ED6 ED09, ED11, ED12, ED15 were used.

5 CONSIDERATIONS ON LEVEL-1 DATASETS

A limited number of evaluation studies of NGRM Level 1 flux datasets have been performed.

- The MTGI-1/NGRM measurements from the selected EDSS electron channels are consistent with the corresponding electron response functions. The derived flux products are in good agreement with the electron flux measurements provided by the NGRM unit on-board EDRS-C.

- The MTGI-1/NGRM measurements from the selected low energy channels present some inconsistencies with the corresponding proton response functions. As a result, the Level 1 proton differential fluxes for E=5.5 MeV are assumed to be underestimated by a factor of 5 while for E=8.5 MeV by a factor of 2, as derived from comparisons with GOES-18/SGPS proton data.

- Strong contamination effects in electron flux products are expected during SPEs.

- Weak contamination effects in proton flux products are expected during strong electron flux enhancements of the outer belt.

- Data users are advised to consult the available ephemeris (ECI coordinates) and magnetic coordinate (e.g., L, MLT) variables, derived using the UNILIB library [RD10] assuming the IGRF model for the internal, and the quiet Olson-Pfitzer 1977 model for the external magnetic field components